



Technical Section

Evaluating the influence of induced passive torques in the simulation of time-varying human poses

I. Rodriguez^{a,*}, R. Boulic^b^a Applied Mathematics Department, Universitat de Barcelona, Gran via de les corts catalans, 585, 08007 Barcelona, Spain^b Virtual Reality Lab, EPFL, Switzerland

ARTICLE INFO

Article history:

Received 10 November 2007

Received in revised form

12 May 2008

Accepted 15 June 2008

Keywords:

Animation

Human poses

Joint fatigue assessment

Passive torques

Virtual humans

ABSTRACT

In the computerized generation of human poses, it is important to take into account not only the active component of the torque, but also the ligaments and connective tissues which produce a passive torque at the limits of the joint range of motion. We present a fatigue model in which both active and passive torque components are essential parameters integrated in an inverse kinematics animation framework. We then use fatigue evolution to optimize the generated posture. We introduce an hysteresis activation pattern for each joint in order to set, whenever necessary, a fatigue reduction scheme through an active torque reduction constraint. The fatigue reduction scheme analyzes the fatigue level of each individual muscular group; when it is above a given threshold, a statically optimal joint variation is enforced to locally reduce the active torque while still achieving a desired task (e.g. reaching a point in 3D space). For that purpose we integrate the influence of passive/resistive torque in an active torque reduction scheme, allowing either the generation of reactive poses (i.e. an active strategy) or, on the contrary, the adoption of more relaxed ones (i.e. a passive strategy).

© 2008 Elsevier Ltd. All rights reserved.

1. Introduction

Many poses and shifts in pose we adopt daily are performed in an unconscious way. In particular, some postural adjustments arise due to muscle fatigue. In several fields, such as computer animation, virtual reality and ergonomics, there is a need to generate realistic human postures based on the context of a simulation or study. But realism in physiological terms (e.g. fatigue) is sometimes sacrificed for efficiency or aesthetic interests in graphic visualization terms. Physiological studies interpret postural control in different ways; some studies rely on reflex mechanisms [1] while others use the term “strategies” or control pattern generators [2]. It is clear, therefore, that posture generation should exploit synergies between animation techniques and physiologically grounded models.

The human body has more than 700 skeletal muscles and most human movements require these muscles to act in groups rather than as individuals. We present a simplified fatigue model, based on antagonistic muscle groups, motivated by the requirement of joint fatigue assessment in real time. The model is associated with an inverse kinematic (IK) animation system so that fatigue is

evaluated during the performance of IK tasks (e.g. 3D position or orientation constraints). When the fatigue level reaches a threshold, the system reacts by creating a constraint that guides the posture towards to a less tiring state, i.e. a recovery posture. Fatigue reduction is performed by minimizing the joint torque component generated by muscle contractions, also named the joint active torque.

In this paper, we propose two strategies to reduce the active torque. The active strategy aims to reduce the joint active torque amplitude by finding solutions in the middle of the joint range of motion, whereas the passive strategy achieves the same goal by exploiting the passive-resistive torque. The effectiveness of the passive-resistive torque being produced by the ligaments and tendons is significant only in the extrema of the joint range of motion [3]. As a consequence, the postures obtained through this latter strategy are less able to produce active torque. To summarize, the two strategies may lead to postural solutions having contrasted potential in terms of reactivity, i.e. the ability to quickly produce an active torque and movement in general. These two families of solutions may also carry distinct behavioral interpretations (i.e. relaxed vs active postures). For example, a relaxed posture is adopted by a standing person maintaining a conversation, and an active posture is adopted by a policeman controlling traffic in order to ensure a quick reaction.

Our system allows to simulate fatigue at joint level under different conditions (e.g. external loads); therefore, it can be used to predict comfort issues when sustaining certain working

* Corresponding author.

E-mail address: inma@maia.ub.es (I. Rodriguez).¹ Supported by UAH Grant PI2005/083 and partially by the Autonomic Electronic Institutions (TIN2006-15662-C02-01) and Agreement Technologies (CONSOLIDER CSD2007-0022, INGENIO 2010) projects.

postures over a long time. In the ergonomic field, it can help to study the readjustment of common fatiguing tasks and help in workplace design. For reaching tasks, our system may predict what should be the posture adopted by a worker when he feels fatigued. Similarly, in the field of computer animation most postures sustained over a long time looks unbelievable as the viewer feels that it should lead to the fatigue of some joint subset. Our dual active–passive approach can also tune the degree of exploiting the passive torque to modulate how relaxed the recovering posture is.

2. Related work

Several studies including musculoskeletal models or physiological factors as fatigue have been proposed to improve the realism of simulated motion or generated posture. Lee designed a system to generate postures depending on the strength model of the figure [4]. Several motion strategies were defined but the completion of a task was not prioritized while a torque strategy was enforced.

Komura developed a human animation system that sought to minimize muscle action [5]. He applied optimal feed-forward control to key poses for a physiologically based retargetting of the motion. In a later study, he combined Delp's musculoskeletal model and Giat's fatigue model [6] to deal with realistic character animations [7]. Unlike Giat's intracellular pH-based fatigue model, our model of fatigue is mainly based on ergonomic studies which use the maximum holding time that a posture can be maintained and the current holding time.

Crowninshield predicted muscle force by minimizing a specified criterion [8]. Crowninshield's method was modified to take into account the dynamics of the musculotendon in the muscle force prediction [3]. Bioengineering researchers have studied methods to simulate human motion by minimizing some other biological values. Another research approach tried to minimize the jerk [9], while another worked on the minimization of muscle signal change [10]. Uno studied the minimization of muscle force change [11]. A study has solved the redundancy of IK problems by using a criterion of minimum muscle-force change [12].

Hyung used optimization-based dynamics to predict the motion of a virtual human. He minimized the largest normalized joint torque where the function assumed that humans move in such a way to avoid experiencing a large normalized torque at any one joint [13]. Our research, as will be seen in the subsequent sections, also relies on this latter fact, since the most fatigued joint triggers a posture adjustment in order to minimize joint active torque.

3. The role of torques in the fatigue model

Our approach splits each single degree of freedom joint into two coordinated half-joints, representing the action of antagonistic groups of muscles. It is important to make this distinction, since the strength of each muscle group differs and depends on the posture. A detailed description of the half-joint concept can be found in [14]. Next, we describe the aspects of the fatigue model.

The basic parameters are the joint strength, joint torque and maximum holding time. The joint strength can be characterized as the maximum torque corresponding to the maximum capacity that a group of muscles has to produce force (muscular strength). We have based our joint strength model on Chaffin results [15]. Thus, for each joint, the normalized torque T_N is calculated as the

ratio of joint torque τ and joint strength st :

$$T_N = \tau / st \quad (1)$$

The current torque τ applied to a joint is expressed as the sum of internal torques, τ_i , and external torques τ_e .

$$\tau = \tau_i + \tau_e \quad (2)$$

Internal torque includes active, τ_a , and passive ones τ_p :

$$\tau = (\tau_a + \tau_p) + \tau_e \quad (3)$$

An active torque is driven by activation patterns mainly initiated in the central nervous system to counter-balance external loads and the influence of the body mass. Ligaments, connective tissues and bone contact induce passive torques. We have used the exponential model of passive torques in Riener [3].

Fig. 1 illustrates the contribution of torques of an elbow joint for an equilibrium state. An external load produces a corresponding external torque (in black) whose magnitude depends on the distance of the force line of action to the joint axis of rotation. In Fig. 1a this torque is counter-balanced only with an active torque produced by the biceps while in Fig. 1b the equilibrium is achieved only by exploiting the passive torque (gray triple line). In some contexts, the passive torque may act in the same direction as the external torque, inducing a higher active torque to achieve a null total torque (Fig. 1c). It is important to note that the direction of passive torque is opposite at both extremes of the joint range of motion (blue curve in Fig. 3).

As we work under the quasi-static hypothesis, the total torque must be zero:

$$(\tau_a + \tau_p) + \tau_e = 0 \quad (4)$$

Then, the active torque can be expressed as

$$\tau_a = -(\tau_p + \tau_e) \quad (5)$$

Likewise, the external torque τ_e can be obtained by exploiting the principle of virtual work that maps Cartesian forces acting on an effector and body weight into equivalent joint torques.

From these elements we can deduce the normalized torque, T_N , and exploit the general force-time relationship expressed as a regression line, valid for several muscle groups [16]:

$$mht = \exp(2.70 - 0.0448T_N) \quad (6)$$

The maximum holding time mht gives the longest period of time during which the posture can be sustained before reaching an unbearable level of fatigue. The fatigue level simply expresses the ratio of the holding time ht by the maximum holding time mht .

$$fatigue_level = \frac{ht}{mht} \quad (7)$$

As we target the fatigue modeling for slowly evolving human postures over time, we use an incremental expression of this quantity. A complete description of the fatigue model can be found in [14,17].

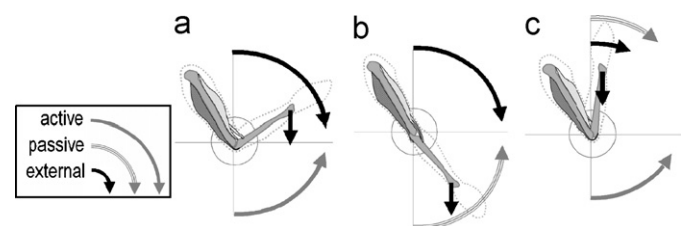


Fig. 1. Three equilibrium configurations with active, passive and external torques.

4. Generating human poses. An IK engine

We have developed a system to simulate human postures. As animation technique, we use IK. The animator generally specifies end-effector (e.g. the hand) and positions constraints (tasks expressed in Cartesian space), and the computer provides the joint configuration needed to achieve the desired task/s. The IK solution² is based on the linearization of the set of equations expressing Cartesian constraints x as functions of the set of degrees of freedom θ . We denote by J the Jacobian matrix gathering the partial derivatives $\partial x / \partial \theta$. We use its pseudo-inverse, denoted J^+ , to build the projection operators $P_{N(J)}$ on the kernel of J , denoted $N(J)$. Our approach relies on an efficient computation of projection operators that allows us to split the constraints set into multiple constraint subsets associated with an individual strict priority level [18].

The provided solution guarantees that a constraint associated with a high priority is achieved as far as possible while a low priority constraint is optimized only on the reduced solution space that does not perturbate all higher priority constraints. For example, such an architecture is particularly suited for the off-line evaluation of the space a virtual worker can reach; in such a context the balance constraint is given the highest priority while gaze and reach constraints have distinct, lower priority levels [19].

5. Constraint system for fatigue reduction

In this section, we describe a constrained solution which incorporates active and passive torques in a fatigue minimization process. A previous study on IK minimized the torques due to gravity by reducing the lever arm of body segments' weight [20]. A subsequent extension included external forces [18]. Its purpose was to converge to postures while minimizing the joint torques. Both of them exploited postural redundancy to solve the optimization problem while controlling some effectors in the Cartesian space. However, the main weakness of these approaches is that the minimization is achieved at the lowest priority level.

Our approach exploits the possibility of introducing strict equality and inequality constraints in the joint space prior to search for the IK solution described in Section 4. These can be named "hard constraints" as they have to be ensured with a higher priority than all other IK tasks. Section 5.1 explains "how" fatigue constraint is computed and Section 5.2 describes "when" it is activated/deactivated, i.e. the activation pattern for each half-joint (equivalent to one muscle group) to set a fatigue reduction constraint whenever a fatigue threshold is exceeded.

5.1. Inequality constraint definition

To better understand the inequality constraint construction, let us recall the definition of a hyperplane $H : H = \{\theta \in \mathbb{R}^n / a^T \theta = b, b \in \mathbb{R}\}$, where a^T represents the normal of the hyperplane H . A hyperplane divides space into lower H_L (green region in Fig. 2) and upper H_U (red region in Fig. 2) half-spaces:

$$\begin{aligned} H_L &= \{\theta \in \mathbb{R}^n / a^T \theta < b, b \in \mathbb{R}\}, \\ H_U &= \{\theta \in \mathbb{R}^n / a^T \theta > b, b \in \mathbb{R}\} \end{aligned} \quad (8)$$

We want to construct an inequality constraint of the form: $a^T \theta \leq b$. In Fig. 2, we describe the construction of the inequality constraint with an example in 2D, i.e. we only manage two joints θ_1 and θ_2 , where the hyperplane appears as a line. As can be

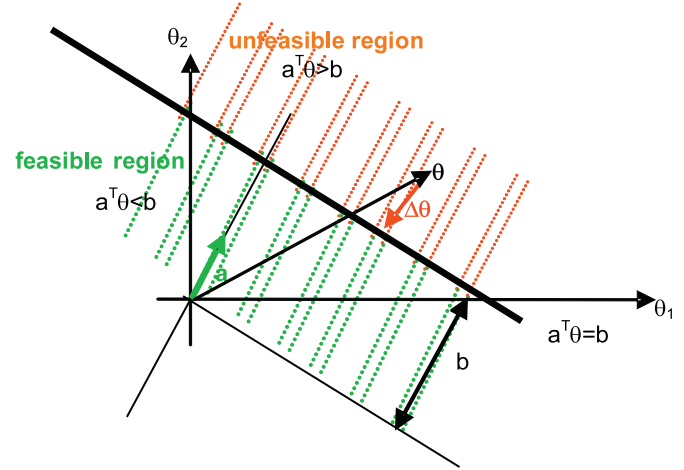


Fig. 2. Example of hyperplane in 2D.

appreciated in the figure, the current vector of joint coordinates, θ , is on the unfeasible region (red dotted region), so a joint variation vector (red arrow) $\Delta\theta$ is needed to drive it to the feasible region (green dotted region). Note that $\Delta\theta$ has the opposite direction to the gradient of the hyperplane, a^T (green arrow):

$$a^T = -\text{normalized}(\Delta\theta) \quad (9)$$

As $\theta + \Delta\theta$ is on the hyperplane (see line $a^T \theta = b$ line in the figure), its product by a^T gives us the scalar b :

$$b = a^T(\theta + \Delta\theta) \quad (10)$$

As seen in formulas (9) and (10), to calculate a^T and b we need to compute the joint variation vector $\Delta\theta$ that will be used to reduce the fatigue level. With this aim in mind, Section 5.1.1 first introduces the muscle action strategy characterizing how the active torque can be reduced. Section 5.1.2 then describes the algorithm that gives us the goal angle with reduced active torque. Finally, Section 5.1.3 uses the algorithm's output to compute the joint variation vector $\Delta\theta$.

5.1.1. The muscle action strategy

The joint variation for fatigue reduction is determined by acting on the contributions of both external and passive torques. Reducing the absolute value of the contribution of the internal torque is the traditional approach chosen for such a problem. Instead, we offer the capability, if desired, to increase the absolute value of the passive torque produced by tendons and ligaments, with the aim of reducing the resulting active torque.

The muscle action strategy aims to simulate the active participation of muscles or, on the contrary, to simulate the passive contribution of muscles and other tissues [21,22]. An active strategy strives to find a solution close to the midrange of the joint where the muscle group is able to produce its active torque efficiently, τ_a . Such a region can also be characterized by a quasi-null passive resistive torque ($\tau_p \sim 0$, see Fig. 3). The passive strategy only exploits the joint passive torque to compensate the action of the external torque. Such a solution is always in the neighborhood of the joint limits, resulting in less reactive/responsive muscles groups because muscle forces are small even for a high degree of activation.

In the scenario in Fig. 3, only the elbow joint is allowed to move. Three postures with a null active torque are highlighted (with a photo below, see the brown line reaching a null torque value). The one in the central joint range is the active solution as it maximizes the muscle activation efficiency while the other two are purely passive/resistive, hence less responsive.

² The research of the inverse kinematics engine supported by the Swiss National Science Foundation.

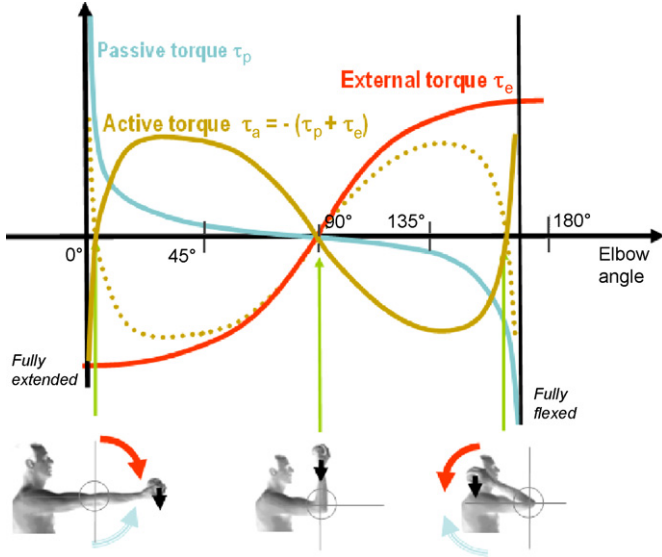


Fig. 3. Frontal elbow case study, the passive torque (blue), the external torque (red), the resulting active torque (brown) and minus active torque (dotted brown).

5.1.2. Reduced active torque algorithm

Relying on the muscle action strategy defined in the previous section, we propose an algorithm to reduce active torque which is hybrid in the sense that it combines the local knowledge of the external torque τ_e (we know only its value for the current joint angle and its current partial derivatives with respect to the joint angles, τ_e value for others joint angles is extrapolated) and the full knowledge of the passive-resistive torque characteristic (τ_p is a known function of the joint state) [23]. Indeed, in the general case, the number of joints considered can be arbitrarily large leading to an unknown variation of the external torque at the individual joint level. In the quasi-static context, we can simply evaluate its current value τ_e , by means of the principle of virtual work, saying that the Jacobian transpose maps Cartesian forces acting at an end-effector into equivalent joint torques, and its current first derivative, $d\tau_e$. As a direct consequence, the algorithm we propose exploits only a linear extrapolation of the external torque based on this information.

We also assume we know the passive torque function τ_p (over the full joint range from the biomechanics literature [3], with anatomic Euler angle convention). As a side remark, in the case study illustrated in Fig. 3 the external torque is induced by the gravity, and the only joint that moves is the elbow. This allows us to draw the external torque function (i.e. the red curve); however, only the local knowledge of the external torque is exploited by the algorithm.

In addition to the specification of the strategy type—active vs passive—the active strategy selects its solution based on a normalized quantity called the active torque decrease ratio R characterizing the quality of the optimized active torque. We have:

$$R = (\tau_a - \tau_{a_min}) / \tau_a \quad (11)$$

where τ_a represents the current active torque, τ_{a_min} is the estimated local minimum of the active torque amplitude, when it exists, in addition to the null global minima achieved with the passive strategy.

When τ_{a_min} is null, a 100% active torque decrease ratio is achieved. This is the ideal case. In other less optimal cases smaller values of R are achieved. For this reason, the active strategy accepts a threshold level R_{min} on this quantity (potentially user-defined). Whenever R is smaller than R_{min} then the solution

provided by the active strategy is not accepted and the algorithm switches to the always-existing extremal passive solution. For example, an R_{min} value of 0.9 means that the user agrees to have compensation of only 90% because the remaining 10% of active torque is a bearable amplitude. This favors solutions lying in the midjoint range characterizing a more reactive posture, even if they are not fully optimal in terms of amplitude.

Table 1 details the algorithm providing the angle θ_g with reduced active torque. Its input is the current joint state θ_c , the active strategy Boolean, the current values of τ_e , τ_p and τ_a , the current first derivative of the external torque $d\tau_e$ and of the passive torque $d\tau_p$ (tabulated), and the threshold R_{min} .

The algorithm based on the current joint state, τ_e , $d\tau_e$, tries to find in the $-\tau_p(\theta)$ curve slopes matching the current external torque derivative.

No matching implies a passive solution located on joint extremes. In this case, the solution is given by a dichotomic function allowing us to find the goal angle θ_g where the external torque line extrapolation intersects with the opposite of the passive torque function (dotted curve in Fig. 4). Two search variants, depending on the sign of $\tau_a(\theta)$, $\tau_a(\theta_{s_min})$, $\tau_a(\theta_{s_max})$, DSS (dichotomic same sign) and DOS (dichotomic opposite sign) are detailed in Table 2.

Whenever two slopes match the current value of external torque derivative, the angles corresponding to those slopes are named θ_{s_min} and θ_{s_max} . We work under the hypothesis of the monotony of the passive torque function (as seen in Fig. 3), the pair of angles are on both sides of the joint angle for which the derivative of the passive torque is minimum (e.g. situated in

Table 1
Minimum active torque search algorithm

```

Search slopes for  $\theta_{d\tau_p}(-d\tau_e)$  // given  $d\tau_e$ , search for the angle/s where  $d\tau_p = -d\tau_e$ 
if no or only one slope{
  if ( $|\tau_a| < \epsilon_\tau$ )  $\theta_g = \theta_c$  //CASE 1.1
  else if ( $\tau_a > \epsilon_\tau$ )
     $\theta_g = \text{Dichotomy}(\theta_{min}, \theta_c, \theta_g)$  //CASE 1.2
  else
     $\theta_g = \text{Dichotomy}(\theta_c, \theta_{max}, \theta_g)$  //CASE 1.3
}
else {/two slopes
  if ( $|\tau_a| < \epsilon_\tau$ ) // equality tolerance see Fig. 4
    {  $\theta_{s\_min}, \theta_{s\_max}$  is the pair of angle values for which  $d\tau_p = -d\tau_e$ 
      if ( $(\theta_{s\_min} < \theta_c < \theta_{s\_max})$  or [ $(\theta_c < \theta_{s\_min}$  or  $\theta_c > \theta_{s\_max})$ 
        and ( $\text{sign}(\tau_a(\theta_{s\_min})) = \text{sign}(\tau_a(\theta_{s\_max}))$ ))
           $\theta_g = \theta_c$  //CASE 2.1
        else{
          if (active) //CASE 2.2
             $\text{Dichotomy}(\theta_{s\_min}, \theta_{s\_max}, \theta_g)$ 
          else  $\theta_g = \theta_c$  //CASE 2.3
        }
    }
  else // ( $|\tau_a| > \epsilon_\tau$ )
    {
      if ( $\text{sign}(\tau_a) = \text{sign}(\tau_a(\theta_{s\_min}))$  and  $\text{sign}(\tau_a(\theta_{s\_min})) = \text{sign}(\tau_a(\theta_{s\_max}))$ )
        {  $\tau_{a\_min}$ : value of the estimated  $\tau_a$  minima
          if ( $\tau_a > 0$ )  $\theta_{\tau_{a\_min}} = \theta_{s\_max}$  else  $\theta_{\tau_{a\_min}} = \theta_{s\_min}$ 
          if active and ( $(\tau_a - \tau_a(\theta_{\tau_{a\_min}})) / \tau_a > R_{min}$ )
             $\theta_g = \theta_{\tau_{a\_min}}$  //CASE 3.1
          else
             $\theta_g = \text{DSS}((\tau_a, \theta_{min}, \theta_{max}, \theta_{s\_min}, \theta_{s\_max}))$  //CASE 3.2
          }
        else
          {if(active)}
             $\theta_g = \text{Dichotomy}(\theta_{s\_min}, \theta_{s\_max})$  //CASE 3.3
          else
             $\theta_g = \text{DOS}((\tau_a, \theta_{min}, \theta_{max}, \theta_{s\_min}, \theta_{s\_max}))$  //CASE 3.4
          }
    }
}

```

the central region in Fig. 3). The algorithm uses both angles to find a partial solution minimizing active torque when both are on the same side (both above or both below) of the external torque extrapolated line (red line in Figs. 6 and 7). In the opposite case in which both angles are on different sides (one above and one below) of the extrapolated line a central solution is found. In other words, τ_a at both angles has the same sign or different sign (see orientation of black arrows in Figs. 6 and 7).

In any case, if the current joint angle is placed in the equality tolerance region, i.e. between the two small dotted curves in Fig. 4, the current angle is considered as the goal angle.

The following figures illustrate the different cases of the hybrid minimization contemplated by the algorithm. Fig. 5a is a case

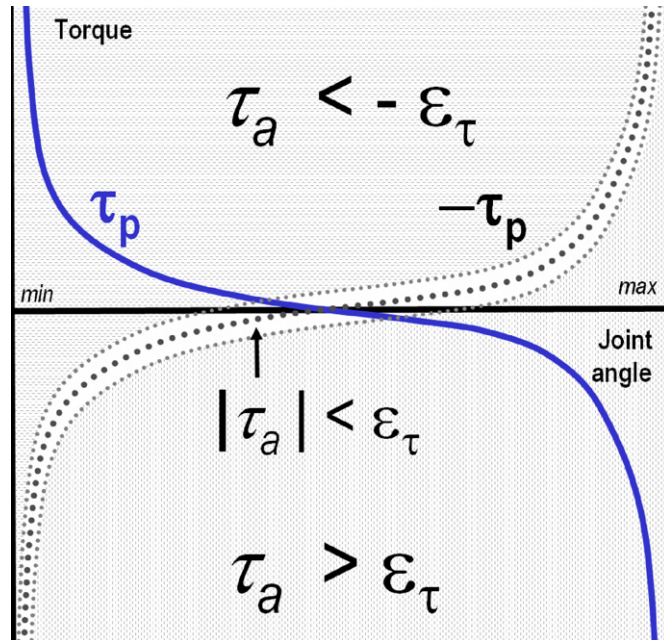


Fig. 4. Sign of τ_a with equality tolerance ϵ_τ .

where no active solution can be found as no slope in the function $-\tau_p$ matches $d\tau_e$. A passive solution is found by dichotomy (intersection of the external torque line with the opposite of the passive torque function). Fig. 5b illustrates the equality approximation; the current state is already optimal.

In Fig. 6 too the current state belongs to the equality approximation but this time the joint angle is smaller than θ_{s_min} . Therefore, one more sign test is required to determine whether another joint angle, closer to the midrange, exists. One is found only in Fig. 6b because the active torque changes sign between θ_{s_min} and θ_{s_max} , while this is not the case for Fig. 6a.

Fig. 7 illustrates cases where the current active torque is not null (e.g. a downward black arrow indicates a negative value). In Fig. 7a the two angles θ_{s_min} and θ_{s_max} , with the same slope as $d\tau_e$ indicate extrema of the active torque variation (with constant sign), the minimum amplitude being obtained for θ_{s_min} . In Fig. 7b the active torque changes sign between θ_{s_min} and θ_{s_max} . If the strategy is active a search is conducted within this interval; otherwise, the closest solution is found.

5.1.3. Building the fatigue reducing joint variation

We have relied on evidences obtained in a study that developed a strength based discomfort model applied to postures and movements [24]. An interesting result of that study is that the total discomfort value indicated for a complete movement is closely connected to the maximal value given for a single body part, i.e. it is not a mean value of different discomfort values inside different body parts. Based on this finding we focus on the most fatigued joint, further indexed with l , to adjust the posture. The vector $J_{\tau_{e_l}}$ gathers the partial derivatives of its external torque τ_{e_l} with respect to all joints:

$$J_{\tau_{e_l}} = \left\{ \frac{\partial \tau_{e_l}}{\partial \theta_j} \right\}_{j=1 \dots n} \quad (12)$$

Its scalar component $\partial \tau_{e_l} / \partial \theta_l$ for the fatigued joint l is the constant external torque derivative $d\tau_e$ used in the general algorithm from Table 1.

To compute $J_{\tau_{e_l}}$, we need the Jacobians J_{T_i} associated with the external forces f_i and the gravity Jacobian J_G associated with the weight w . This is the expression of the partial derivative

Table 2
Functions defining intervals of dichotomic search (general algorithm—cases 3.2 and 3.4)

```

DSS( $\tau_a, \theta_{min}, \theta_{max}, \theta_{s\_min}, \theta_{s\_max}$ ) = Dichotomy(SameSignMinandMax( $\tau_a, \theta_{min}, \theta_{max}, \theta_{s\_min}, \theta_{s\_max}$ ),  $\theta_g$ )
SameSignMinandMax(input:  $\tau_a, \theta_{min}, \theta_{max}, \theta_{s\_min}, \theta_{s\_max}$ , output: SameSignMin, SameSignMax)
{
  if ( $\tau_a > \epsilon_\tau$ ) //  $\tau_e$  is below the curve  $-\tau_p(\theta)$ 
  { SameSignMin =  $\theta_{min}$ , SameSignMax =  $\theta_{s\_min}$  }
  else //  $\tau_e$  is above the curve  $-\tau_p(\theta)$ 
  { SameSignMin =  $\theta_{s\_max}$ , SameSignMax =  $\theta_{max}$  }
}

DOS( $\tau_a, \theta_c, \theta_{min}, \theta_{max}, \theta_{s\_min}, \theta_{s\_max}$ ) = Dichotomy(OppoSignMinandMax( $\tau_a, \theta_c, \theta_{min}, \theta_{max}, \theta_{s\_min}, \theta_{s\_max}$ ),  $\theta_g$ )
OppoSignMinandMax(input:  $\tau_a, \theta_{min}, \theta_{max}, \theta_{s\_min}, \theta_{s\_max}$ , output: OppoSignMin, OppoSignMax)
{
  if ( $\tau_a > \epsilon_\tau$ ) //  $\tau_e$  is below the curve  $-\tau_p(\theta)$ 
  {
    if ( $\theta_c < \theta_{s\_max}$ ) { OppoSignMin =  $\theta_{min}$ , OppoSignMax =  $\theta_{s\_min}$  }
    else { OppoSignMin =  $\theta_{s\_max}$ , OppoSignMax =  $\theta_{max}$  }
  }
  else //  $\tau_e$  is above the curve  $-\tau_p(\theta)$ 
  {
    if ( $\theta_c > \theta_{s\_min}$ ) { OppoSignMin =  $\theta_{s\_max}$ , OppoSignMax =  $\theta_{max}$  }
    else { OppoSignMin =  $\theta_{min}$ , OppoSignMax =  $\theta_{s\_min}$  }
  }
}

```

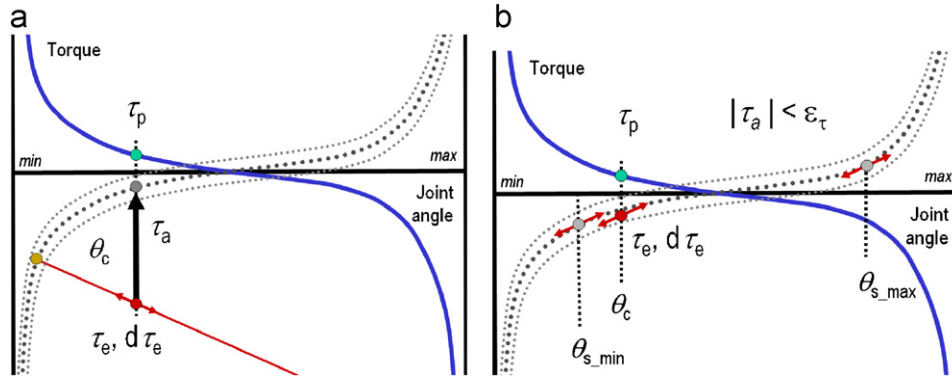


Fig. 5. (a) Case 1.2: no slope in $-\tau_p$ matching $d\tau_e$. (b) Case 2.1: $(|\tau_a| < \epsilon_\tau)$ and $(\theta_{s_min} < \theta_c < \theta_{s_max})$.

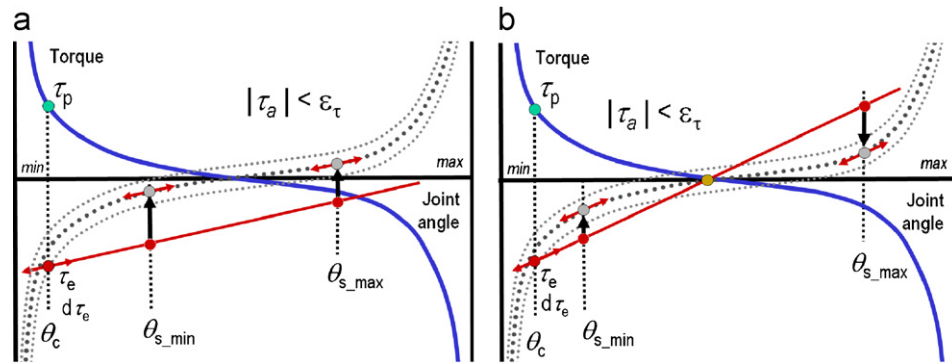


Fig. 6. (a) Case 2.1: $(|\tau_a| < \epsilon_\tau)$ and $(\theta_c < \theta_{s_min}$ or $\theta_c > \theta_{s_max})$ and $\text{sign}(\tau_a(\theta_{s_min})) = \text{sign}(\tau_a(\theta_{s_max}))$. (b) Cases 2.2, 2.3: $(|\tau_a| < \epsilon_\tau)$ and $(\theta_c < \theta_{s_min}$ or $\theta_c > \theta_{s_max})$ and $\text{sign}(\tau_a(\theta_{s_min})) \neq \text{sign}(\tau_a(\theta_{s_max}))$.

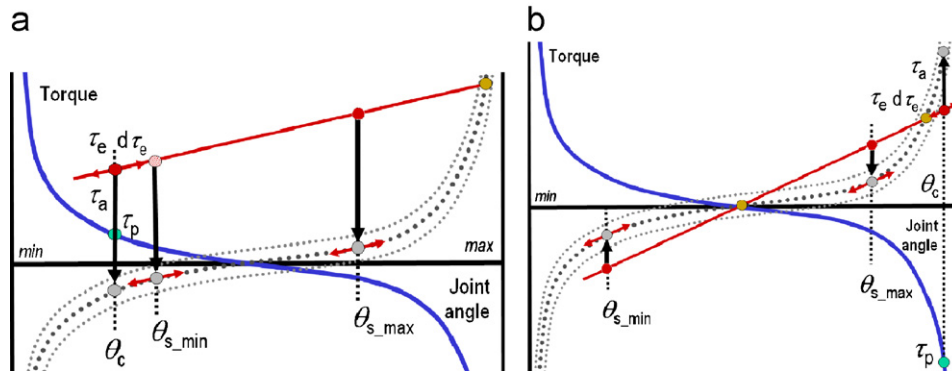


Fig. 7. (a) Cases 2.3, 3.2: $(|\tau_a| > \epsilon_\tau)$ and $(\text{sign}(\tau_a) = \text{sign}(\tau_a(\theta_{s_min})))$ and $(\text{sign}(\tau_a) = \text{sign}(\tau_a(\theta_{s_max})))$. (b) Cases 3.3, 3.4: $(|\tau_a| > \epsilon_\tau)$ and $(\text{sign}(\tau_a) \neq \text{sign}(\tau_a(\theta_{s_min})))$ or $(\text{sign}(\tau_a) \neq \text{sign}(\tau_a(\theta_{s_max})))$.

corresponding to the joint j :

$$\frac{\partial \tau_{e_l}}{\partial \theta_j} \sum_{i=1}^{ne} J_{T_i} (f_i \times r_j) + J_{G_l} (w \times r_j) \quad (13)$$

where ne is the number of external forces, J_{T_i} is the column l of J_{T_i} , J_{G_l} is the column l of J_G associated with the weight w , and r_j represents the unit axis of rotation of joint j . We need only the column l of these Jacobians because it corresponds to the external torque of the most fatigued joint.

We have then all the information we need for the reduced active torque algorithm (Section 5.1.2) to obtain a target joint

angle θ_g for the most fatigued joint (component $\Delta\theta_l$ of the fatigue reducing posture variation).

$$\Delta\theta_l = \min(\beta(\theta_g - \theta_c), \Delta\theta_{max}) \quad (14)$$

where θ_g is the current joint angle, β is a positive number smaller than 1 for stability and $\Delta\theta_{max}$ is a small amplitude required to preserve the validity of first order approximation of this non-linear system.

The other components of the posture variation $\Delta\theta$ are obtained from the gradient of the cost function $h_\tau(\theta) = \|\tau_{e_l}\|^2$ given by $\nabla h_\tau(\theta) = 2 \cdot \tau_{e_l} \cdot J_{T_l}^T$ where τ_{e_l} is the external torque of the most fatigued joint and $J_{T_l}^T$ is the Jacobian gathering the partial

derivatives of the torque function $\tau_e(\theta)$ with respect to all joint angles. Then, the joint variation for all of the joints, apart from the most fatigued one (already formulated in 14), states as follows:

$$\Delta\theta_j = \alpha \cdot \nabla h_{\tau}(\theta) \quad \text{for } j \neq l \quad (15)$$

where α is a negative scalar and $\nabla h_{\tau}(\theta)$ is the gradient of the cost function h trying to minimize the influence of the external torque for the most fatigued joint.

5.2. Inequality constraint activation by hysteresis

The fatigue reduction constraints are managed by hysteresis thresholding which forces a minimal duration for the recovery by setting a lower threshold for de-activating constraints; this reflects human behavior better than a single activation/deactivation threshold [25]. When a half-joint fatigue level is above the fatigue threshold, the fatigue constraint produces a joint variation, as defined in the previous section, locally reducing the half-joint torque by a small increment compatible with the simulation time increment. Therefore, the IK animation system converges incrementally from the fatigue posture towards the rest posture; while the other IK tasks are achieved in the null space of that constraint. The constraint exists until the half-joint recovery level is reached (second line of arrows in Fig. 8), at which time the fatigue constraint is deactivated. When multiple joints are in a fatigued state, the first one that reaches a fatigue threshold will be the one responsible for triggering a fatigue minimization constraint.

Fig. 9 shows hysteresis behavior during a simulation using a skeleton with colored muscles representing the fatigued group of muscles, in this case, the biceps. At the instant of time T0, the virtual human adopts the initial posture. At T1, he moves towards the goal situated over the oblique line. At T2, the goal is reached. At T3, the subject maintains the posture and a significant fatigue value is reached. This is clear from the intense red color in the bicep muscle. Fatigue increases even more until T4. At T5 when fatigue reaches a predefined threshold, the posture is adjusted in order to reduce fatigue. At this moment (see Fig. 8) a fatigue reducing constraint is activated. At T6, the posture allows a decrease in the fatigue level. This is clear from the less intensive red color in the muscle. Once recovered, the fatigue constraint is deactivated (see Fig. 8). Then, from T7 to T8 the arm moves towards the goal again.

We have set two tasks with different priorities. The high-level priority task is to attract the effector (square in Fig. 10) to reach

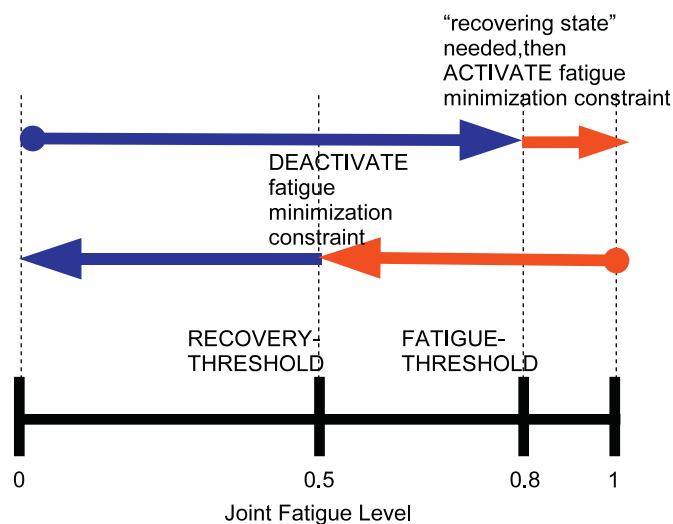


Fig. 8. Constraint hysteresis activation pattern.

any point on the oblique line L. It is completed with a lower priority task that tries to also attract the same effector to reach the vertical plane P. As a consequence the posture converges to the intersection of the line L with the plane P as can be seen between the instants T2–T4 in Fig. 9. Then, when the fatigue is too intense, the automatic torque reduction constraint is set. This can be seen as an even higher priority level task compared to the two existing one. As a consequence, the priority level task degrades first to meet the new torque reduction constraint, whereas the line attraction can still be enforced (T5 and T6). When the recovery is achieved the torque reduction constraint vanishes and the posture converges again to the posture achieving both the line and the plane goals.

6. Experiments and simulations

6.1. Experimental design

The objective of the experiment was to explore the positions of recovery subjects found when they felt fatigued after maintaining a posture during a certain time period. The experiment consisted in maintaining the wrist over a line marked on the wall. We wanted to compare the responses achieved by different subjects at different settings of controllable variables such as load weight and line inclination. Afterwards, we made a comparison, in terms of recovery strategies, with computer generated simulations.

The experiment was designed using a replication and blocking technique. We took measures in different subjects in order to be able to generalize any conclusions obtained. The blocking technique was used to divide the observations into blocks (groups) in order to compile data in each group under similar experimental conditions. We defined three groups of experiments: oblique -45° , oblique -25° and horizontal lines.

Fig. 11 depicts the elements used in the experiment. The subject had an orange sphere on the wrist, which projected over a preferred dot on the middle line. A video camera recorded a side view of the subject. The subject looked at a monitor situated in front of him. A mirror helped subjects to correct their posture to prevent movements such as abduction. Note that we worked in the sagittal plane. The experiment was performed using 12 male and female aged between 30 and 40. The experiment procedure, corresponding to simulation task in Fig. 10, was explained to the subjects: “Stay in the initial preferred position as long as you can. When you feel fatigue near to exhaustion (i.e. 0.8 on a 0–1 scale), change your posture in order to rest a little while still projecting the sphere on the middle line. If you have recovered sufficiently, i.e. 0.5 on a 0–1 scale, then feel free to move along the line to the preferred position. The experiment stops when you are not able to recover along the blue line”.

6.2. Analysis of data from experiment and simulations

From the video recording, we extracted snapshots of positions of recovery and plotted wrist position over time. Recordings of the oblique -25° case (see Fig. 12) showed that subjects only found one position of recovery, i.e. 1.40 m from the floor to the position of recovery in the oblique line. In the horizontal case (see Fig. 13) the conclusion of the experiment was also that the subjects found only one position to recover from a fatiguing state, i.e. 0.60 m of distance from the shoulder to the position of recovery. In both cases the goal/recovery posture found by the subjects was consistent with an active strategy. Note that both figures show repetitive patterns of recovery and initial postures because the

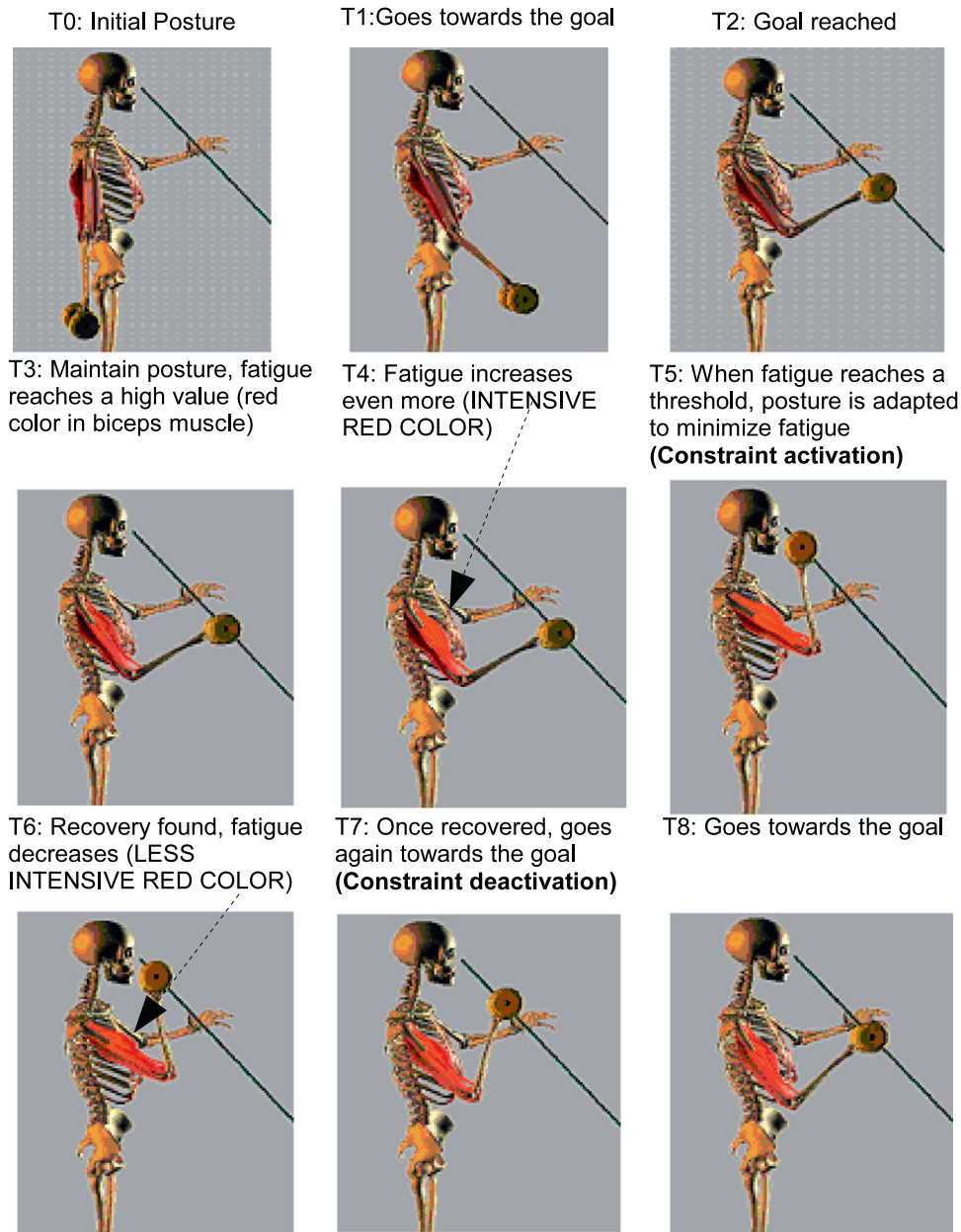


Fig. 9. Fatigue constraint triggering.

subjects were instructed to repeat the fatigue/recovery process until they no longer found rest along the blue line.

The oblique -45° case showed that subjects found two positions of recovery. One position, characterized by an active strategy, is the same as in the previous horizontal and oblique -25° cases (continuous arrow in Fig. 14). Nevertheless in this case some subjects adopted a second position of recovery trying to move downward to find rest (discontinuous arrow in Fig. 14); subjects later reported that they did not know why. An explanation, supported by our muscle action strategy, is that the downward movement leads to a temporary decrease in the active muscle effort as long as the height of the arm's center of mass decreases the potential energy of the arm.

From Figs. 15 to 17 we present simulation results as an active torque vs joint angle plot where the two snapshots of the virtual human show the initial posture, i.e. the posture producing fatigue, and the goal posture, i.e. the posture where recovery is found. The goal posture is obtained by adjusting the initial one by means of the reduced active torque algorithm

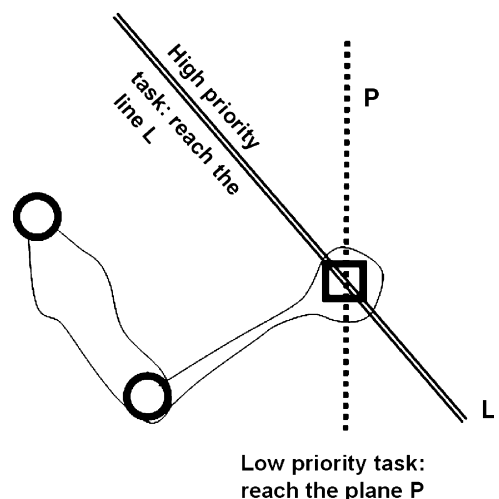


Fig. 10. Tasks definition.

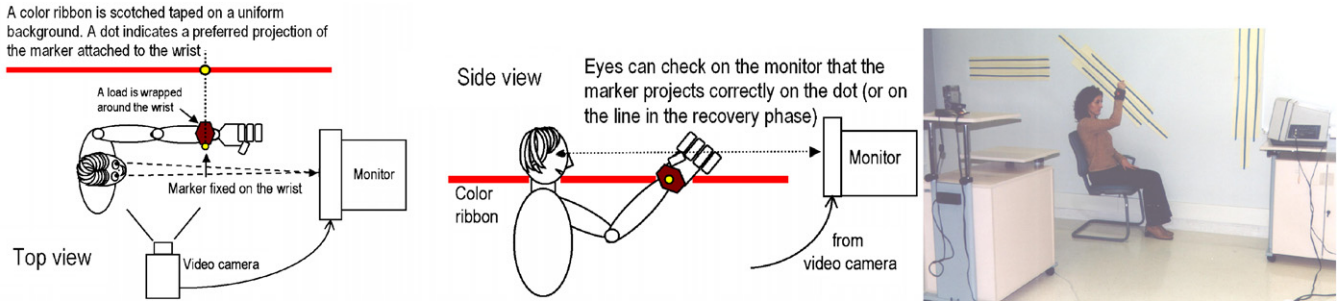


Fig. 11. Experiment layout.

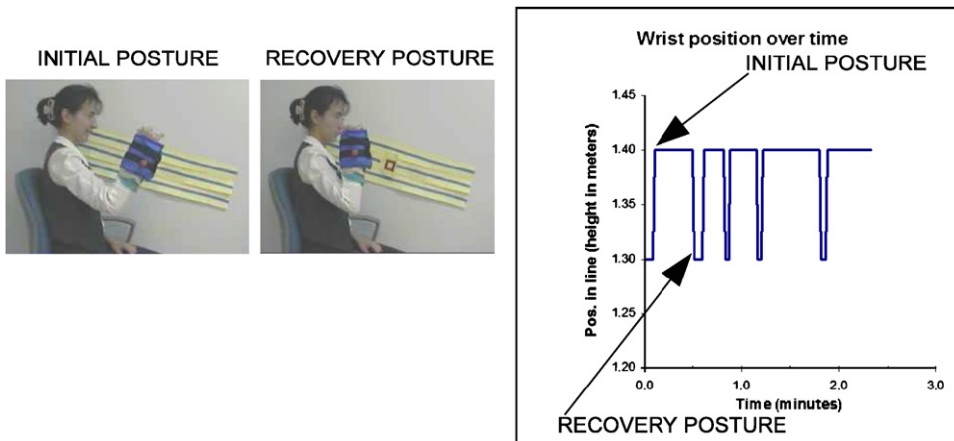


Fig. 12. Experiment in the oblique -25° case. Load 2.5 kg.

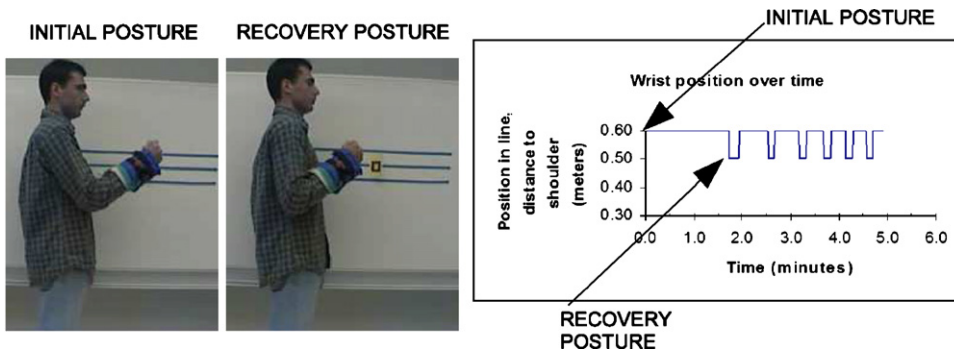


Fig. 13. Experiment in the horizontal case. Load 2.5 kg.

and the joint variation forced by an inequality constraint (detailed in Section 5). During the simulation, the wrist is constrained on an oblique line, both shoulder and elbow joints are allowed to move, and the one with the highest fatigue value will launch the fatigue inequality constraint. According to fatigue and recovery scales used during the experiment, the simulation fatigue threshold was set to 0.8 and recovery threshold to 0.5 (recall Fig. 8).

Fig. 15 shows the shoulder adopting a passive strategy, shoulder active torque at the beginning of the simulation was about 7.5 Nm, and after the iterative execution of the IK engine driven by a fatigued constraint, the joint achieved a partial reduction of active torque. We call this a passive strategy because the joint finds some recovery (active torque reduction and in consequence partial fatigue decreasing) in the neighborhood of

the joint limits (i.e. between 0° and 15°). In the experiments the equivalent behavior to this passive solution also seemed to be insufficient (i.e. a partial fatigue decrease) because the subject had to correct the passive strategy by continuing with an active one (as shown by the arrows in Fig. 14).

Fig. 16 shows simulation results for an active strategy with ratio $R = 0, 2$, i.e. the user agrees with a 20% of active torque decrease. In this simulation the most fatigued joint, due to the selected initial posture, is the extensor muscle group. The same results are obtained for a passive strategy because the algorithm does not find slope matching (see the first group of cases contemplated by the algorithm in Table 1).

Fig. 17 presents simulation results also in the case of no slope matching in the reduced active torque algorithm, but in this case the most fatigued joint is the shoulder joint. There is a

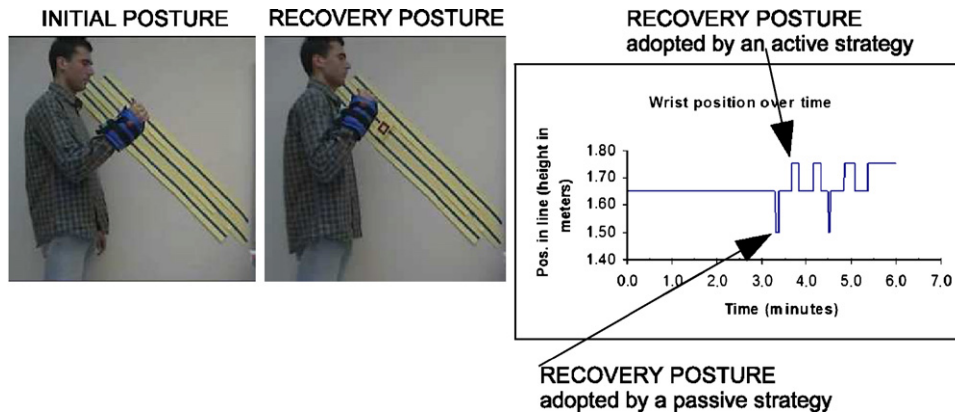


Fig. 14. Experiment in the oblique -45° case. Load 2.5 kg.

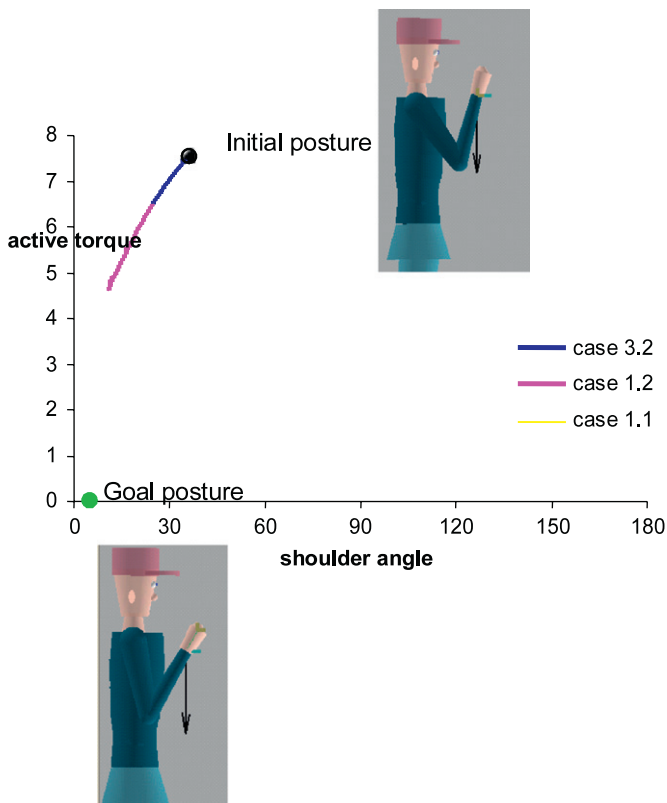


Fig. 15. Passive strategy simulation.

discontinuity, i.e. a sudden change in active torque value, near the lower limit of the shoulder range of movement; this is because the passive torque function has been reshaped only in the neighborhood of the joint limits. The reshape is done using a small linear term added on both limits to ensure that passive torque is big enough to compensate external torque. Then, passive torque near the limit becomes substantially larger than in the middle of the joint range and active torque value is affected by this change in passive torque value.

7. Conclusions and future work

We have designed and implemented a fatigue model not at individual muscular level, but at joint level exploiting antagonistic muscular groups. It can be applied for gradually changing

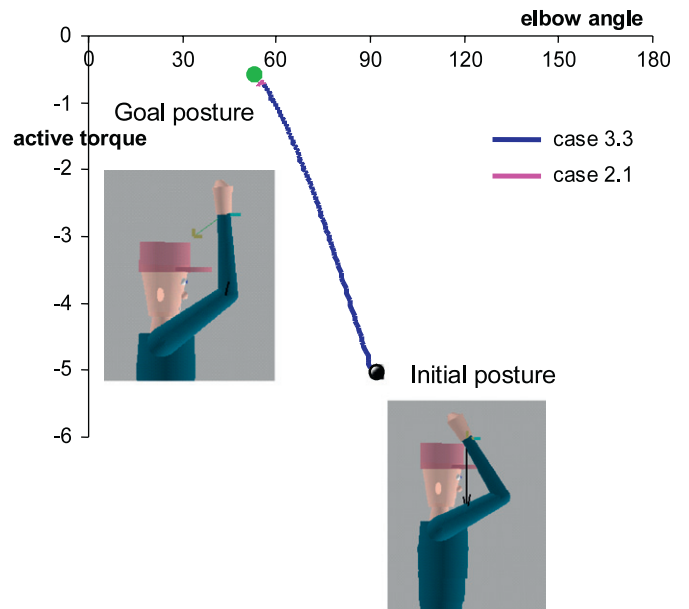


Fig. 16. Active strategy simulation with $R = 0.2$.

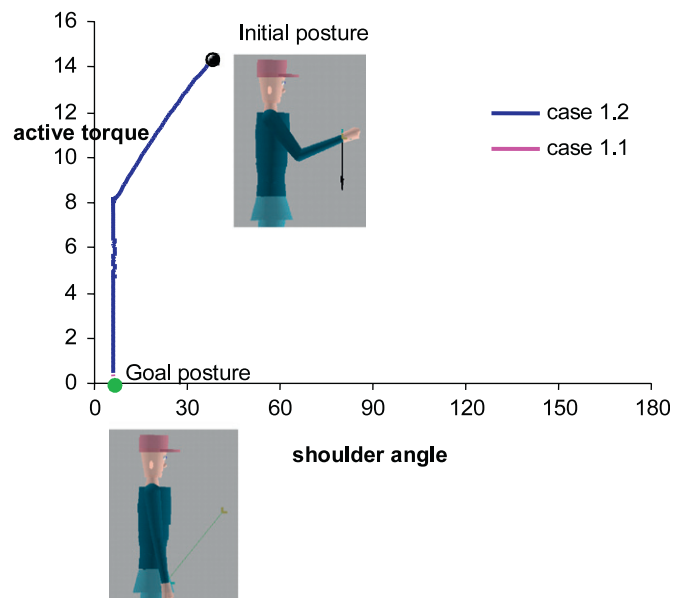


Fig. 17. Active strategy with $R = 1$ and a passive strategy.

postures. It is a generic model that can be applied to different muscular groups of the human body. Its main contributions are the reduced number of parameters used and the consideration of the pass of time in the model. The fatigue model has been exploited in an inverse kinematics framework for realistic posture generation. During the simulation, joints fatigue values are updated so that the system reacts when unbearable fatigue values are reached. The fatigued posture is then adjusted, searching for a less fatigued one.

The possibility of using several constraints and ordering them by priority has allowed us to enforce the importance of some constraints next to others. We have designed a general and hybrid algorithm that clearly delineates all the cases where a solution can be found in the direction reducing the joint active torque amplitude (active strategy) or in the direction of the always existing passive-resistive solution. We do not use a minimization technique like gradient descent as it exploits local knowledge of external and passive torque, and cases where the derivative is null provide no solution. Our approach can infer from the current state whether it is possible to find an active solution. If it is not possible the passive solution is provided. The algorithm only makes the small assumption that the passive-resistive torque function is a monotonously decreasing function over the joint range. We have also introduced a user-given parameter, named the minimal active torque decrease ratio R_{min} that leads us to accept a partial decrease in the active torque amplitude compatible with the fatigue recovery [26].

We have conducted an experiment to study the fatigue minimization strategy, in other words, the recovery strategy, adopted by subjects loading a weight while being constrained to follow a target line. Specifically, we stated three types of lines to follow: horizontal, -25° oblique and -45° oblique lines. We have observed that the subjects adopted an active strategy when the potential energy of the system remains constant, for example, when the line to move along a horizontal line. However, in an oblique line task context, a minority of attempts were favoring a temporary release of the arm potential energy corresponding to a passive strategy. Both behaviors can be simulated by our inverse kinematic animation system exploiting the proposed reduced active torque algorithm. So the algorithm gives insight into how people readjust fatigued postures and can be integrated in real time applications for the postural control of virtual humans.

An issue for future research is the extension from slowly evolving postures to a dynamic case. The consideration of dynamic constraints (position, orientation, balance) with dynamic properties such as priority, would help to achieve complex postures and so contribute to the adjustment of fatigued postures. Under fatigued conditions, we may also take advantage of the environment to find rest. For example, when arm joints are too fatigued, a postural change may find rest in objects in the scene, a table, a chair, etc. For instance, elderly people getting into a car would represent an interesting case study.

References

- [1] Dietz V. Human neuronal control of automatic functional movements: interaction between central programs and afferent input. *Physiological Reviews* 1992;72:33–69.
- [2] Macpherson JM. Changes in postural strategy with interpaw distance. *Journal of Neurophysiology* 1994;71:931–40.
- [3] Riener R, Edrich T. Identification of passive elastic joint moments in the lower extremities. *Journal of Biomechanics* 1999;32:539–44.
- [4] Lee PLY, Wei S, Zhao J, Badler N. Strength guided motion. *Computer Graphics* 1990;24(4):253–62.
- [5] Komura T, Shinagawa Y, Kunii TL. Muscle based feed-forward controller of the human body. *Computer Graphics Forum* 1997;16(3):165–76.
- [6] Giat Y, Mizrahi J, Levy M. A musculotendon model of the fatigue profiles of paralyzed quadriceps muscle under FES. *IEEE Transactions on Biomedical Engineering* 1993;40(7):664–74.
- [7] Komura T, Shinagawa Y. Attaching physiological effects to motion-captured data. In: *Graphics interface proceedings*; 2001. p. 27–36.
- [8] Crowninshield RD, Brand RA. A physiologically based criterion of muscle force prediction in locomotion. *Journal of Biomechanics* 1981;14:793–800.
- [9] Flash T, Hogan N. The coordination of arm movements: an experimentally confirmed mathematical model. *Journal of Neuroscience* 1985;5(7):1688–703.
- [10] Kawato M. Optimization and learning in neural networks for formation and control of coordinated movement. *Attention and Performance* 1992;XIV:821–49.
- [11] Uno Y, Suzuki R, Kawato M. The control model that establish trajectories similar to those by the brain—the minimum muscle-force-change model. In: *The fourth symposium on biological and physiological engineering*; 1989. p. 299–302.
- [12] Komura T, Shinagawa Y, Kunii TL. An inverse kinematics method based on muscle dynamics. In: *Proceedings of computer graphics international*; 2001. p. 15–22.
- [13] Hyung JK, Horn E, Jasbir S, Abdel-Malek K. An optimization-based methodology to predict digital human gait motion. In: *Digital human modeling for design and engineering symposium*, Iowa, USA, June 2005.
- [14] Rodriguez I, Boulic R, Meziat D. A joint-level model of fatigue for the postural control of virtual humans. In: *Human and computer 2002*, Tokyo, Japan; 2002. p. 220–5.
- [15] Chaffin DB. *Occupational biomechanics*. New York: Wiley; 1988.
- [16] Manenica I. A technique for postural load assessment. In: Corlett N, Manenica I, Wilson J, editors. *The ergonomics of working postures*. London: Taylor & Francis; 1986. p. 271–7.
- [17] Rodríguez I. Joint-level fatigue simulation for its exploitation in human posture characterization and optimization. PhD thesis; 2004.
- [18] Baerlocher P, Boulic R. An inverse kinematic architecture enforcing an arbitrary number of strict priority levels. In: *The visual computer*, vol. 20(6). Berlin: Springer; 2004.
- [19] Boulic R, Baerlocher P, Rodriguez I, Peinado M, Meziat D. Virtual worker reachable space evaluation with prioritized inverse kinematics. In: *35th international symposium on robotics*, Paris; 2004.
- [20] Boulic R, Mas R, Thalmann D. Complex character positioning based on a compatible flow model of multiple supports. *IEEE Transactions on Visualization and Computer Graphics* 1997;3(3):245–56.
- [21] Esteki A, Mansour JM. An experimentally based nonlinear viscoelastic model of joint passive moment. *Journal of Bio-mechanics* 1996;29(4):443–50.
- [22] Hatze H. A three-dimensional multivariate model of passive human joint torques and articular boundaries. *Clinical Biomechanics* 1997;12:128–35.
- [23] Rodriguez I, Boulic R. Simulating reactive/passive postures by means of a human active torque hybrid minimization. In: *International conference on computer graphics theory and applications*; 2007. p. 5–12.
- [24] Zacher I, Bubb H, Yerkes KL. Strength based discomfort model of posture and movement. *Journal of Aerospace* 2004;113(1):87–92.
- [25] McNally IM. Contrasting concepts of competitive state-anxiety in sport. Multidimensional anxiety and catastrophe theories. *Athletic insight. Journal of Sport Psychology* 2002;4(2) [on line].
- [26] Boulic R, Mas R, Thalmann D. A robust approach for the center of mass position control with inverse kinetics. *Journal of Computers and Graphics* 1996;20(5).